Clays and Clay Minerals, Vol. 46, No. 3, 290–300, 1998.

REACTIVITY OF BASAL SURFACES, STEPS AND EDGES OF MUSCOVITE: AN AFM STUDY

Z. Z. ZHANG[1] AND G. W. BAILEY[2]

[1] National Research Council, % U.S. Environmental Protection Agency, 960 College Station Road, Athens, Georgia 30605-2700

[2] Ecosystems Research Division, National Exposure Research Laboratory, U.S. Environmental Protection Agency, Athens, Georgia 30605-2700

Abstract—The reactivity of basal surfaces, steps and edges of muscovite was studied by imaging surface precipitates of $PbCl_2$ using atomic force microscopy (AFM). We reacted $PbCl_2$ solution with freshly cleaved muscovite surfaces and found that $PbCl_2$ precipitates were formed on the basal surfaces, steps and edges. It was observed that $PbCl_2$ precipitated preferentially along the steps compared to the basal surfaces and that $PbCl_2$ precipitates at multiple-layer edges were needle-shaped and oriented in different directions. One of the muscovite samples we cleaved had muscovite fragments sitting on the freshly cleaved surfaces. These fragments resulted from previously formed cracks. Thus, we were able to compare the reactivity of the weathered surfaces with that of freshly cleaved surfaces. It was found that $PbCl_2$ was not precipitated along the edges of previously cracked muscovite fragments. These results clearly demonstrated that the edges of freshly cleaved muscovite are the most reactive surface sites, whereas the edges of weathered muscovite are not as reactive. We believe that the surface reactivity of the edges of freshly cleaved muscovite is likely due to terminal $Al\text{-}OH_2^{1/2+}$ or $Al\text{-}OH^{1/2-}$ groups on these crystalline surfaces, which favor adsorption of Pb^{2+} ions and the subsequent nucleation and precipitation reactions. We also investigated the effect of drying rate on the morphology of the surface precipitates. Fast drying resulted in a nearly complete covered surface with a leaflike morphology, whereas slow drying resulted in more isolated surface clusters.

Key Words—AFM, Morphology, Muscovite, Precipitation, Reactivity, Surfaces.

INTRODUCTION

The reactions of metals with surfaces of soil minerals greatly affect their distribution, speciation, transport, toxicity, fate and bioavailability in natural terrestrial and aquatic environments. The significance of adsorption–desorption and precipitation–dissolution reactions in regulating the behavior of trace metals is widely recognized (Stumm and Morgan 1995). The reactions of heavy metals at mineral surfaces are shown to be a continuum from monolayer adsorption of metal ions to cluster formation or multilayer adsorption and, finally, heterogeneous surface precipitation, which in turn can mask the properties of the underlying mineral surfaces (Bleam and McBride 1985; Davis and Hem 1989; Fendorf et al. 1992; O'Day et al. 1994).

The surfaces of soil minerals are generally heterogeneous. Surface heterogeneity has been observed directly using various experimental techniques. Hochella et al. (1989) observed the surface heterogeneity of hematite and galena at nanometer as well as atomic scale using scanning tunneling microscopy (STM). Surface heterogeneity plays an important role in various surface reactions (Hochella 1990). Atomic steps, edges, kink sites, dislocations and point defects are important in controlling many mineral-solution reactions, such as crystal growth and mineral dissolution (Dibble and Tiller 1981; Lasaga 1981). The sorption-site heterogeneity of mineral surfaces has been observed by Lee and Jackson (1977) using a ^{235}U fission particle tracer method, which revealed that uranyl complexes (UO_2^{2+}) adsorbed preferentially at micaceous mineral edges and optically visible steps. Jean and Bancroft (1985) observed, using scanning electron microscopy (SEM), that Au deposition occurred preferentially at the edges of sulfide minerals. These observations suggest that the edge sites of these minerals are more reactive than basal surfaces for the adsorption and nucleation reactions. Mineral surfaces may also act as a template for the epitaxial growth of solid precipitates when the structure of the solid precipitates resembles that of the substrate minerals. Therefore, fundamental knowledge on surface reactivity will improve our understanding of the mechanisms of surface reactions and enhance our ability to predict the behavior of heavy metals in the environment.

The invention of AFM by Binnig et al. (1986) has been a major breakthrough in surface science, allowing scientists in many fields to obtain unprecedented information on the nanometer-scale structure, topography and morphology of surfaces of conductors and insulators under a variety of conditions. Images of sample surfaces may be obtained in vacuum, in air, in water or other liquids. Unlike traditional microscopes, which use wave property of light or electrons to create a 2-dimensional projection of the subject, AFM can

routinely produce 3-dimensional images with nanometer-scale resolution. Under optimized conditions, AFM is able to achieve atomic resolution. For example, Ohnesorge and Binnig (1993) obtained images of the *1014* cleaved plane of calcite underwater, showing the arrangements of surface oxygen atoms, single atomic steps as well as atomic-scale defects on steplines. However, according to Binnig (1992), the interpretation of AFM images with atomic resolutions is further complicated by the fact that the apex of an AFM tip is not likely to be a single atom, but rather consists of several atoms which act like minitips. When minitips are present, although atomic resolution is still possible, the image is actually produced by superposition of multiple images and the interference between them. These individual images, while nearly identical, are phase-shifted with respect to each other. Consequently, only periodic structure can be observed clearly, whereas nonperiodic structures and defects in periodic structures are very difficult to resolve. Thus, most results at atomic resolution have been obtained on layered structures along well-defined atomic planes, such as graphite, boron nitride and micas (Binnig 1992). These complications do not apply when AFM is used to determine surface structures that are larger than the apex of the tip (Binnig 1992). Therefore, AFM is expected to make major contributions in areas of research that involve larger surface dimensions.

Recently, AFM has been employed in a number of studies to examine the surface reactivity and surface reactions, such as adsorption/desorption, oxidation/reduction and precipitation/dissolution of trace metals on surfaces of minerals such as goethite and silica (Fendorf et al. 1996), hematite and albite (Junta and Hochella 1994), brucite (Jordan and Rammersee 1996), calcite (Dove and Hochella 1993) and gypsum (Bosbach and Rammersee 1994). Fendorf et al. (1996) found that Cr(III) precipitates are evenly distributed over goethite surfaces, but form discrete clusters on silica surfaces. They attributed the difference in surface morphology to the difference in bond distance between sorbate and sorbent. Junta and Hochella (1994) studied Mn(II) oxidation at mineral surfaces of hematite and albite. They found that steps are the most reactive sites for initiating the adsorption–oxidation reactions and that the continued adsorption–oxidation process is mineral-surface dependent, resulting in 2 types of growth mechanisms, namely, substrate- and precipitate-controlled growth.

In this study, we employ AFM to examine the surface reactivity of muscovite by imaging surface precipitates of $PbCl_2$. We focused our research on examining the reactivity of basal surfaces, steps and edges of muscovite. In addition, we also determined the effect of drying rates on the morphology of surface precipitates. Thus, we are able to compare surface morphologies that result from a near-equilibrium process with those from a kinetically-controlled process and to gain a better understanding of the mechanisms of surface precipitate formation.

MATERIALS AND METHODS

Muscovite obtained from Ward's Natural Science Establishment Inc. (Rochester, New York) was cut into square pieces of ~1 cm^2 and glued on AFM sample disks. The muscovite samples were then cleaved using Scotch tape. Aliquots of 20 to 50 μL of 2 solutions having concentrations of 5×10^{-5} *M* and 5×10^{-4} *M* $PbCl_2$ were pipetted onto the freshly cleaved muscovite samples. The pH values of these 2 solutions were initially 4.75 and 4.50, respectively, and they were not adjusted during our experiments. The speciation of Pb(II) in the $PbCl_2$ solutions under our experimental conditions was calculated using the MINTEQA2 model (Allison et al. 1991). The muscovite samples were then either air-dried at room temperature under covered petri dishes (slow-drying process) or vacuum-dried in a desiccator (fast-drying process). The slow-drying process took about 48 h, whereas the fast-drying process took less than 1 h.

AFM images of the dried muscovite samples were obtained using a NanoScope III atomic force microscope manufactured by Digital Instruments (Santa Barbara, California). We employed the standard contact mode using 225-μm-long etched silicon cantilevers. All images reported here are shown as scanned and have not been altered or enhanced. During the sample scans, both the high-pass and low-pass filters were turned off. The distribution of the $PbCl_2$ precipitates formed on the various surface sites provided graphic evidence about the reactivity of these surfaces. The reactivity of basal surfaces can be evaluated from perfectly cleaved muscovite sample surface, whereas the reactivity of basal surfaces versus that of steps and edges can be compared from imperfectly cleaved muscovite samples. One of the muscovite samples we cleaved had muscovite fragments sitting on the freshly cleaved surfaces. These fragments are most likely derived from previously weathered cracks. Thus, we are able to compare the reactivity of weathered surfaces with that of freshly cleaved surfaces. Finally, we examined the effect of drying rate on the morphology of surface precipitates formed on perfectly cleaved muscovite samples.

RESULTS AND DISCUSSION

Reactivity of Basal Surfaces, Steps and Edges of Freshly Cleaved Muscovite

Circular-shaped $PbCl_2$ precipitates were found on the basal surfaces, steps and edges of an imperfectly cleaved muscovite (Figure 1a). The pH of $PbCl_2$ solutions was not adjusted during our experiments. The speciation of Pb calculated using MINTEQA2 model

https://doi.org/10.1346/CCMN.1998.0460308 Published online by Cambridge University Press

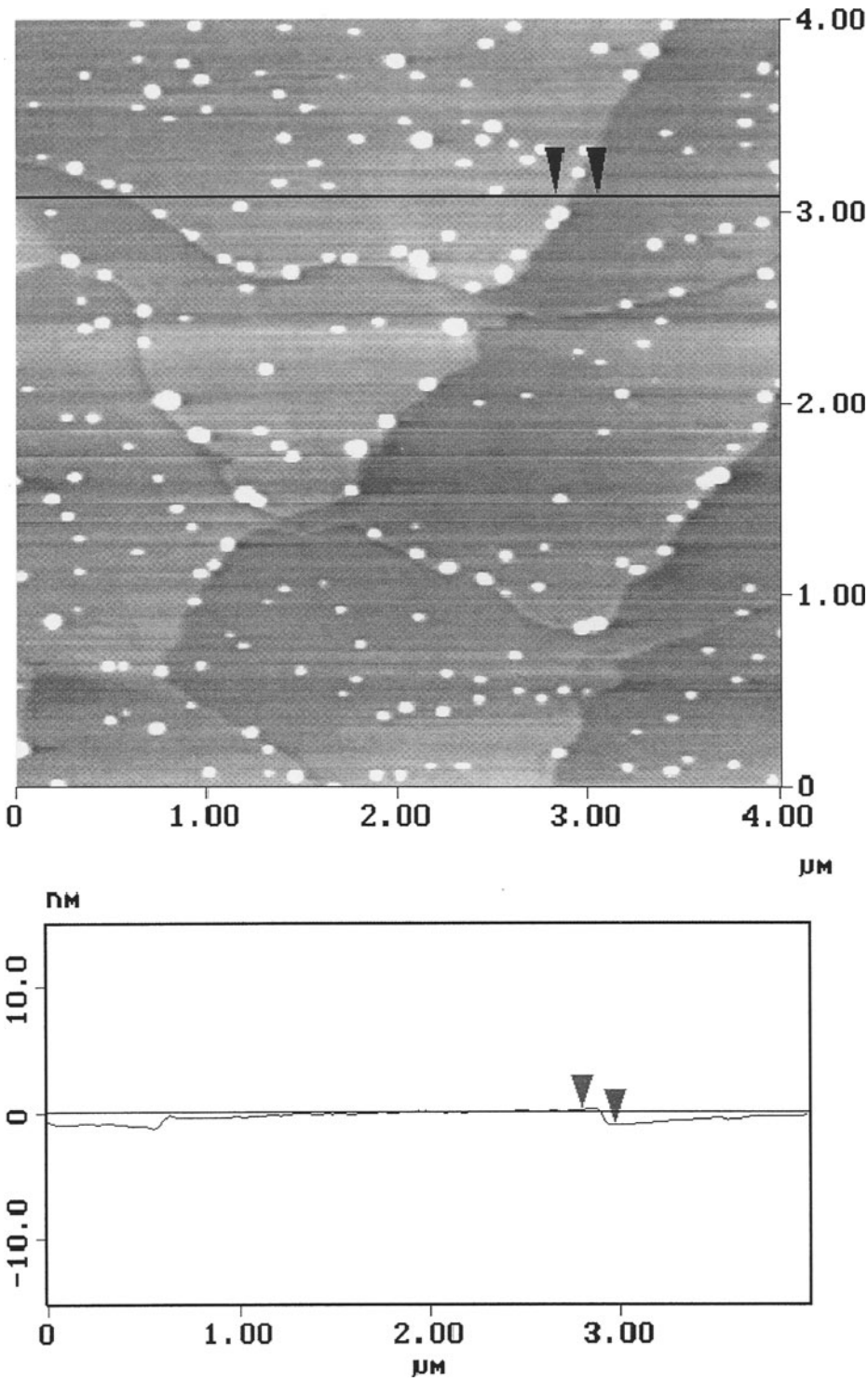

Figure 1. a) Circular-shaped precipitates of $PbCl_2$ on an imperfectly cleaved muscovite surface: 40 μL 5×10^{-5} *M* $PbCl_2$ solution pipetted onto a muscovite sample ~1 cm^2 in surface area and air-dried in a covered petri dish. Note the terraces of atomically flat basal surfaces (001 planes) and broken steps and edges, mainly in the direction from upper right to the lower left, and the preferential precipitation of $PbCl_2$ along these broken steps compared to the terrace surfaces. b) A trace along the cross section as marked by the line in (a) is shown. The height of the step in this image is measured to be ~1 nm, showing a step of a single mica layer.

https://doi.org/10.1346/CCMN.1998.0460308 Published online by Cambridge University Press

(Allison et al. 1991) showed that 99.5% of the Pb(II) is in the form of Pb^{2+}. Therefore, only a small fraction of Pb^{2+} ions were hydrolyzed and lead hydroxide and carbonate were not expected to form. From material balance consideration, we believe that the surface precipitates shown in Figure 1a and subsequent figures are essentially $PbCl_2$. In addition, recent results in our laboratory showed that the morphology of surface precipitate of lead carbonate hydroxide ($Pb_3(OH)_2(CO_3)_2$) differs from that shown in Figure 1a and subsequent figures (Zhang and Bailey 1997).

It can be seen clearly from Figure 1a that terraces of atomically flat basal surfaces *(001)* and broken steps and edges are oriented mainly in the direction from upper right to the lower left. A step height measurement (Figure 1b) showed that the step consists of a single mica layer of ~1 nm. In addition, it is clear that the circular-shaped precipitates of $PbCl_2$ along the broken steps grew mainly on the upper terraces (Figure 1a), which is very similar to the nucleation and growth of Fe metal on Cu *(111)* (Brodde and Neddermeyer 1992) and precipitation of Mn(III) oxyhydroxides, which form along the top edges of albite (Junta and Hochella 1994). Furthermore, one sees that $PbCl_2$ precipitates are distributed preferentially on these broken steps compared to the terrace basal surfaces. The reactions are most likely initiated by adsorption of Pb^{2+} ions at sites along the step edges followed by nucleation and precipitation. Thus, our results clearly demonstrate that edges of a single mica layer are more reactive than the basal surfaces. These results are in agreement with earlier findings that uranyl complexes were preferentially adsorbed at micaceous mineral edges and optically visible steps (Lee and Jackson 1977).

Junta and Hochella (1994) showed that the type of surface precipitate shown in Figure 1a is formed by the process of precipitate-controlled growth, suggesting that the surfaces cannot provide the ideal chemical and geometrical match for epitaxial growth of surface precipitates. The features observed in Figure 1a for surface precipitates of $PbCl_2$ are expected based on crystallographic considerations. Lead halides are always anhydrous and have distorted close-packed halogen lattices (Cotton and Wilkinson 1988). Lead chloride (cotunnite) is orthorhombic dipyramidal with a = 4.52, b = 7.61 and c = 9.03 Å, with Pb-Cl distance about 3.0 Å. The Si-O distance in a silicate tetrahedron is 1.62 Å and the O-O distance is 2.64 Å. Therefore, a precipitate of $PbCl_2$ would not be expected to grow epitaxically on the basal surfaces of muscovite.

The image in Figure 2a shows that the precipitates of $PbCl_2$ grow laterally at an edge composed of multiple mica layers. They are needle-shaped and oriented in various directions, ranging from a relatively small angle of ~10° to ~90° relative to the mean plane of the edge. The step height of the edge shown in Figure 2a is ~23 nm, that is, 23 layers of muscovite (Figure 2b). Note that the shapes of the surface precipitates are different for those formed along the large step edges and those formed along the single-layer step edges. A plausible explanation for the shape and orientation of the precipitates at the large step edges is as follows. The step edge of multiple mica layers is not atomically smooth. Instead, a number of crystalline surfaces (*hkl* planes) are exposed at this edge. Broken Si-O-Si bonds at these crystalline surfaces would react with H^+ and OH^- to form Si-OH in an aqueous environment. The pKa of the terminal Si-OH group is estimated to be 9.5 (Jackson 1964). Thus, these Si-OH groups are stable under our experimental conditions and likely not involved in complexing Pb^{2+} ions. Similarly, broken Al-OH-Al bonds would result in either $Al\text{-}OH^{1/2-}$ or $Al\text{-}OH_2^{1/2+}$, depending on the pH of the solution (each hydroxyl is shared by 2 neighboring aluminums in an uninterrupted muscovite layer, and therefore a broken Al-OH bond has a formal charge of 1/2−). The pKa of the $Al\text{-}OH_2^{1/2+}$ group was proposed to be 5.0 (Jackson 1964). Hohl and Stumm (1976) found that Pb^{2+} ions are specifically adsorbed on hydrous aluminum oxide. Therefore, it is reasonable to hypothesize that nucleation, aggregation and precipitation of $PbCl_2$ on muscovite are likely initiated from Pb^{2+} ions adsorbed onto these terminal $Al\text{-}OH_2^{1/2+}$ or $Al\text{-}OH^{1/2-}$ groups. Since these terminal groups on different crystalline surfaces have different orbital orientations with respect to the mean plane of the edge, the precipitation of $PbCl_2$ can be expected to occur along different spatial directions. Scheidegger et al. (1996) conducted an XAFS study and showed that Ni adsorption on pyrophyllite likely occurred via an edge sharing of 2 oxygens (hydroxyls) on the adjacent Al and Ni octahedra or possibly through the formation of mixed Ni-Al hydroxides. However, since Pb-Cl and Al-OH (1.92 Å, Radoslovich 1975) bond lengths differ significantly, mixed Pb-Al compounds are not expected to form on the edges of muscovite.

Reactivity of Edges of Weathered Muscovite Fragments

Figures 3a and 3b show the muscovite fragments resulting from fractures due to previous weathering along with circular-shaped $PbCl_2$ precipitates sitting on the basal surfaces. The muscovite fragments are characterized by the triangular-, rectangular- or pentagonal-shapes and, more importantly, by the presence of perfectly flat basal surfaces. It can be seen clearly that $PbCl_2$ precipitates were not formed along the edges of these muscovite fragments, even though $PbCl_2$ precipitate was formed on the basal surfaces of 1 muscovite fragment (Figure 3b, lower right corner), as evidenced by the pitted precipitate surface. These results indicate that the edges of weathered muscovite are not as reactive as those of freshly cleaved muscovite. The lack

https://doi.org/10.1346/CCMN.1998.0460308 Published online by Cambridge University Press

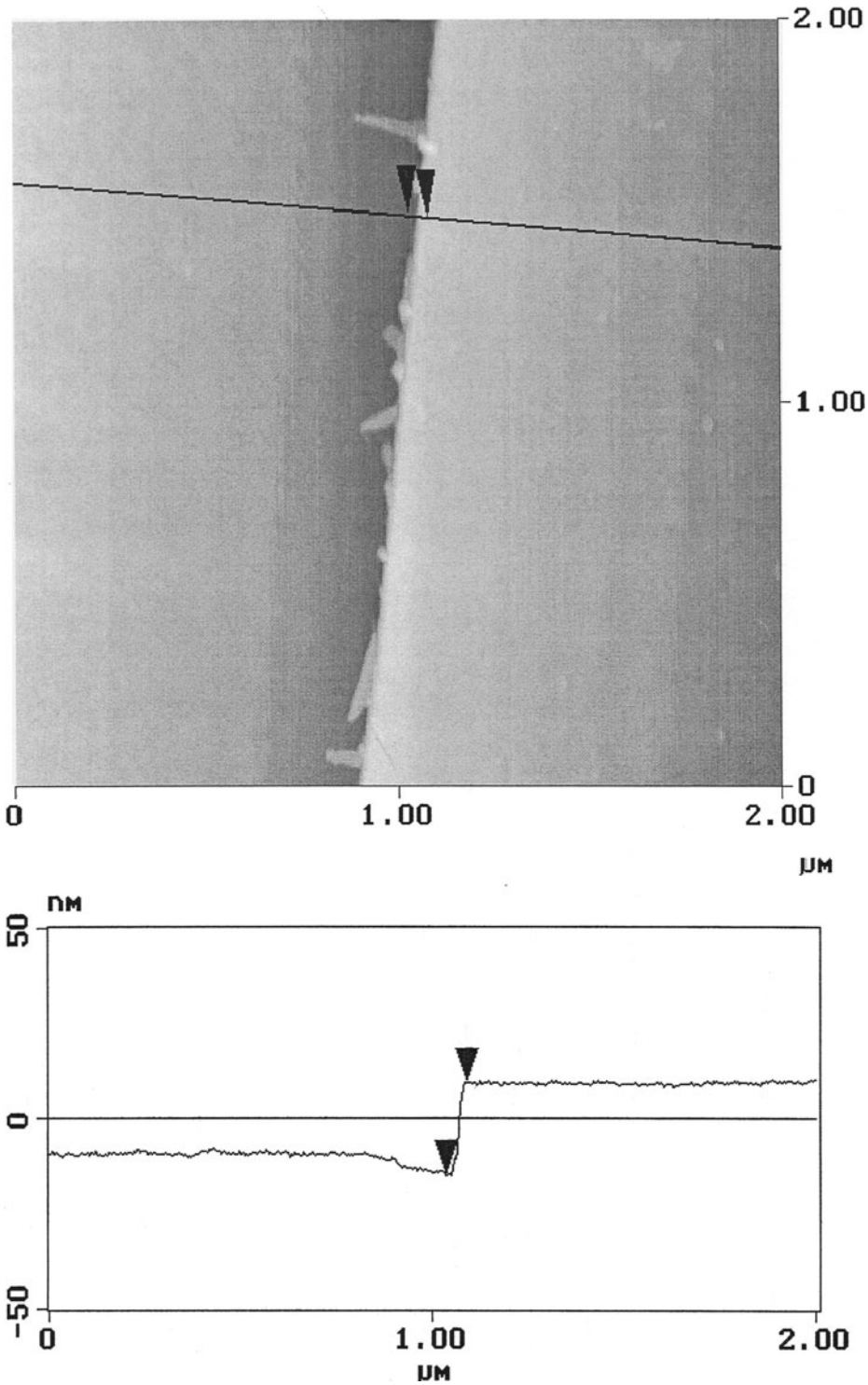

Figure 2. a) Precipitates of $PbCl_2$ at an edge of multiple mica layers: 20 μL 5×10^{-5} *M* $PbCl_2$ solution pipetted onto a muscovite sample ~1 cm^2 in surface area and dried in a desiccator under vacuum. Note that the $PbCl_2$ precipitates formed on the edge are needle-shaped and oriented in different spatial directions. b) A trace along the cross section as marked by the line in (a) is shown. The height of this step is ~23 nm, indicating that the step consists of 23 mica layers.

https://doi.org/10.1346/CCMN.1998.0460308 Published online by Cambridge University Press

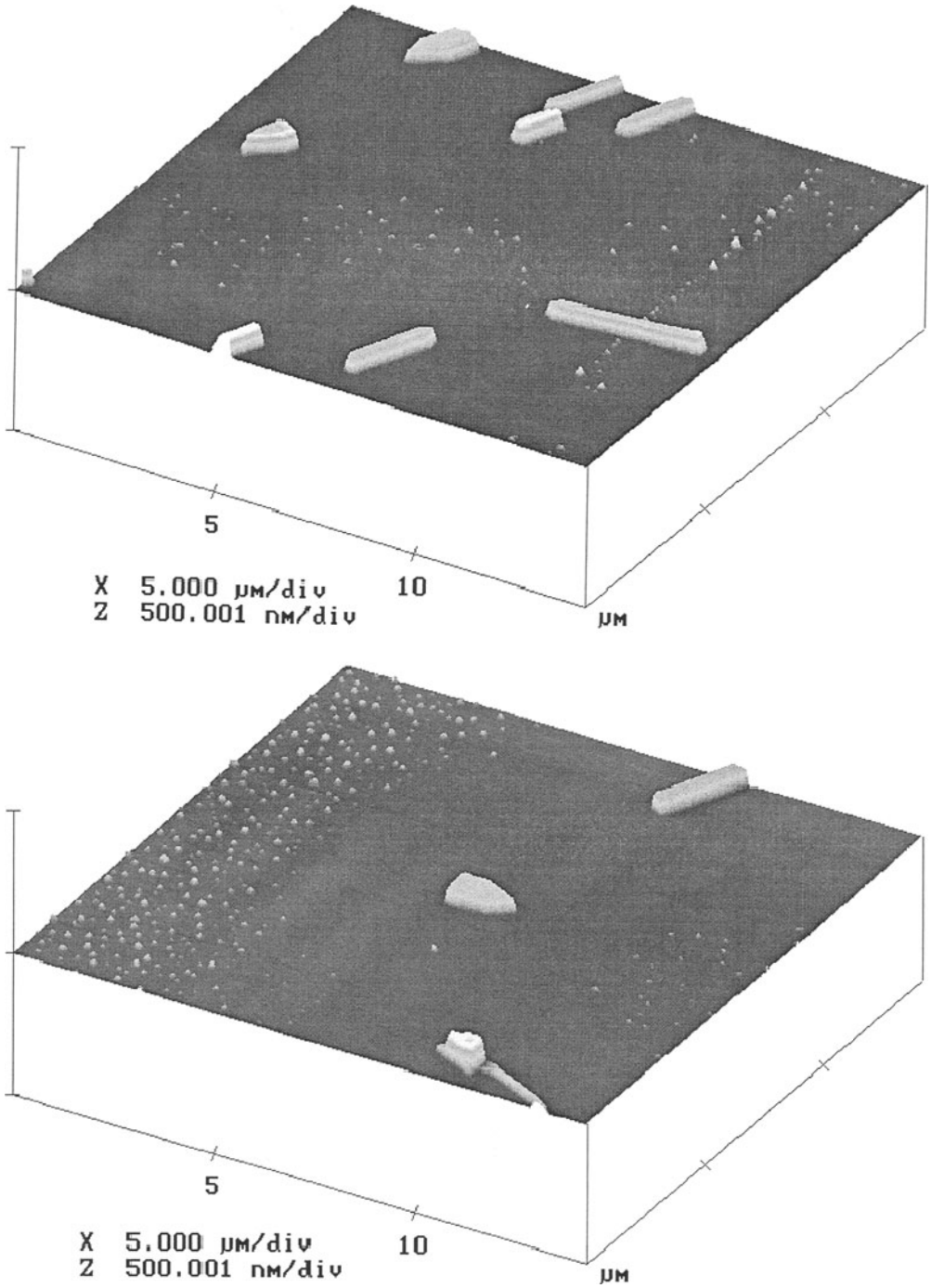

Figure 3. Precipitates of $PbCl_2$ on surfaces of muscovite with cracked muscovite fragments: 20 µL 5 × 10^{-4} *M* $PbCl_2$ solution pipetted onto a muscovite sample ~1 cm^2 in surface area and air-dried in a covered petri dish. a) Image showing that $PbCl_2$ precipitates were not formed along the edges of weathered muscovite fragments. b) Image showing that pitted precipitate of $PbCl_2$ was formed on the basal surfaces of 1 muscovite fragment (near bottom right).

https://doi.org/10.1346/CCMN.1998.0460308 Published online by Cambridge University Press

of reactivity of the edges of weathered muscovite is likely due to inorganic or organic coatings previously formed on these surfaces. This result also provides additional evidence that the most reactive sites on the edges of freshly cleaved muscovite are the broken bonds on these surfaces.

Effect of Drying Rate on the Morphology of Surface Precipitates

The morphology of $PbCl_2$ precipitates on the basal surfaces is affected by the drying rates of the sample. Fast drying of 20 μL of 5×10^{-4} *M* $PbCl_2$ solution resulted in surface regions nearly completely covered with $PbCl_2$ deposits having a leaflike morphology (Figures 4a and 4b). Examination of the 2 images in Figure 4 shows that there are cone-shaped islands in the middle of leaflike precipitates and that the leaflike precipitates appear to be isolated with boundaries or interspersed with smaller circular-shaped precipitate clusters. The same $PbCl_2$ solution, after slow-drying, resulted in isolated circular-shaped surface clusters as shown in Figure 5. Note in these figures that the *z*-axis is extended 10 times relative to the *x*- and *y*-axis to emphasize differences in elevation. Therefore, the real heights of the cone-shaped and circular-shaped precipitates are much lower than what appeared in these figures. It should be emphasized that, regardless of the drying method employed, the solid $PbCl_2$ is deposited very unevenly across the muscovite surface on a macroscopic scale, resulting in areas that are devoid of precipitated $PbCl_2$. The images shown in Figures 4 and 5 are taken from isolated regions on muscovite surfaces on which $PbCl_2$ is found deposited. Thus, the fact that the areal density of precipitated $PbCl_2$ shown in Figures 4a and 4b is obviously much greater than that in Figure 5 has no bearing in the overall material balance that must hold for these systems.

It is obvious from Figures 4 and 5 that the dynamics of the drying process affect the morphology of the surface precipitates. The precipitation reaction in the fast-drying process was far from equilibrium and the surface precipitates in Figures 4a and 4b are metastable compared to these in Figure 5. In the fast-drying process, water rapidly evaporates from the film of $PbCl_2$ solution resting on the muscovite sample. Consequently, the solution quickly becomes supersaturated and $PbCl_2$ precipitates rapidly on the muscovite surfaces. Furthermore, the large value of heat of vaporization of liquid water (ΔH = 44.016 kJ mol^{-1} at 25 °C) can be expected to cause the solution to cool considerably during the fast-drying process, further lowering the solubility of $PbCl_2$. Although the precipitation of $PbCl_2$ is exothermic (the heat of precipitation is estimated to be 13.8 kJ mol^{-1} using the van't Hoff equation and solubility data at 2 temperatures: 0.99 g/100 mL at 20 °C and 3.34 g/100 mL at 100 °C, respectively; Weast and Astle 1982), the total amounts of $PbCl_2$ precipitated are so small that heat released due to precipitation is negligible. Thus, it is reasonable to identify the rapid rate of $PbCl_2$ precipitation resulting from high loss rate of solvent water and the associated cooling as being the principal factor causing $PbCl_2$ to precipitate in the unusual leaflike morphology shown in Figures 4a and 4b. Conversely, it can be argued that the formation of more isolated surface clusters seen in Figure 5 would be expected when conditions where a diffusional mode of material transport operates allowing Pb^{2+} and Cl^- ions in the saturated solution film to preferentially precipitate at nucleation sites distributed across the muscovite surfaces.

The cone-shaped islands, particularly the one located near the center of Figure 4a, are interesting by virtue of their height. They are much higher than the other features shown in Figures 4a and 4b. Furthermore, note that the $PbCl_2$ deposits are partially or completely depleted around the bottom of the cone-shaped islands in the middle of leaflike structures. The large height of the cone-shaped islands and the depletion of materials around their bottom suggest that some nondiffusional mechanism for material transport is involved in their formation. One possibility is capillary flow, or wicking, which could provide a means for the upward flow of saturated $PbCl_2$ solution. Evaporation of solvent water coupled with vertical temperature gradient should generate the necessary condition for the formation of cone-shaped islands shown in Figures 4a and 4b.

A series of concentric rings of $PbCl_2$ were often observed for the slow-drying process. Smaller $PbCl_2$ aggregates were found in the outside ring with increasing particle size toward the center (Figures 6a and 6b). Again, note in these figures that the *z*-axis is extended 10 times relative to the *x*- and *y*-axis. This phenomenon resembles the macroscopic Liesegang rings reported in the colloid chemistry literature (Weiser 1935; Henisch 1988). Liesegang observed the rings of chromate in gelatin jelly when he placed a drop of silver nitrate on a glass plate coated with moist gelatin containing potassium dichromate (Weiser 1935). The formation of Liesegang rings was first accounted for by Ostwald's supersaturation theory (Weiser 1935). The added electrolyte diffused in the gel, reached supersaturation up to a certain point and was followed by rapid precipitation. However, Liesegang ring formation is also observed in systems in the presence of dispersed crystallites (Henisch 1988), in which supersaturation should not occur. Other theories were proposed to account for the Liesegang ring formation, such as competitive particle growth theory and sol coagulation theory (Henisch 1988). The Liesegang rings in the gel were formed from the inside-outward, whereas the surface precipitate rings on the muscovite are formed from the outside-inward. Nevertheless, the underlying principles are similar. The formation of the

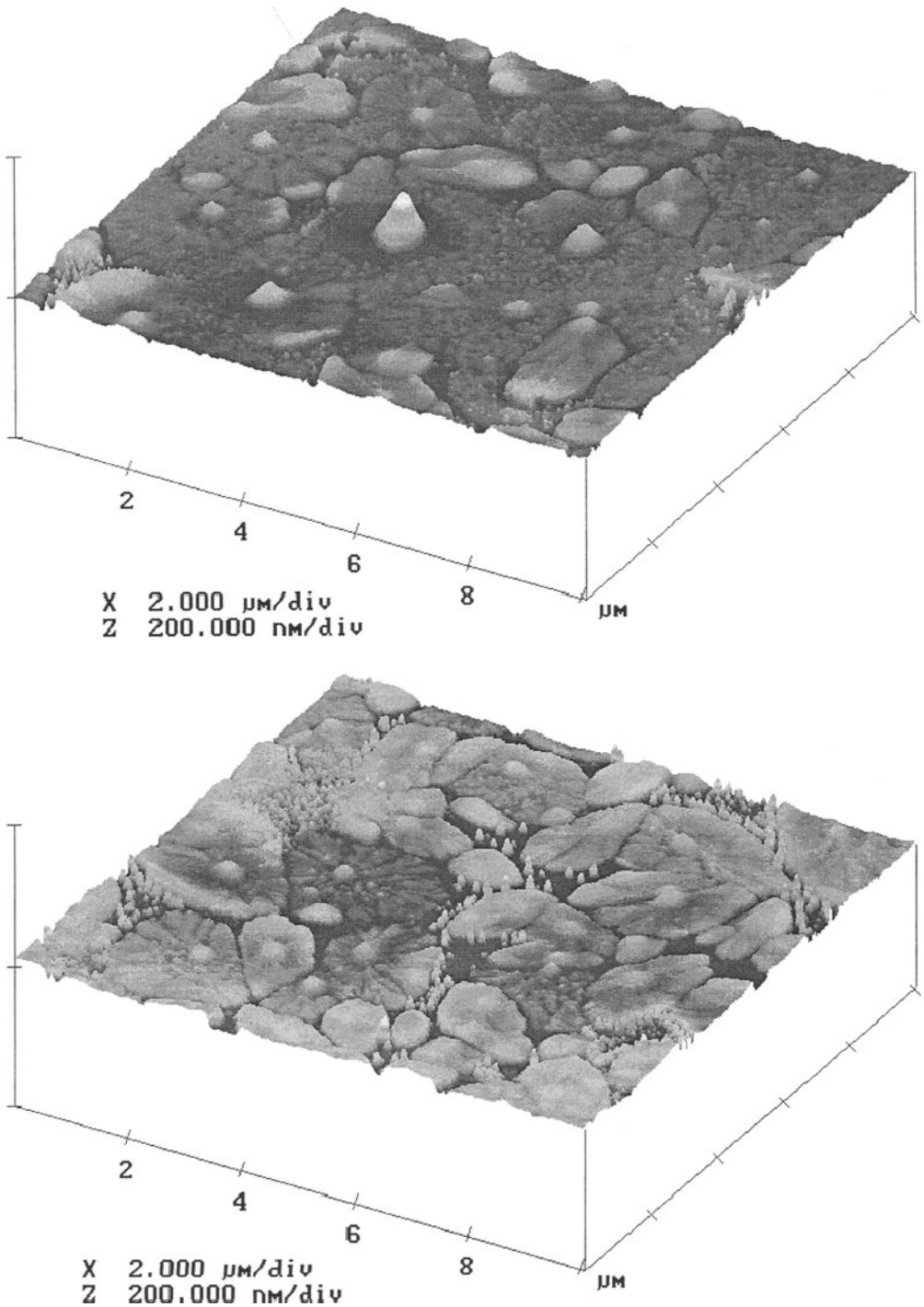

Figure 4. Precipitates of $PbCl_2$ on perfectly cleaved basal surfaces of muscovite (001 plane): 20 μL 5×10^{-4} *M* $PbCl_2$ solution pipetted onto a muscovite sample ~1 cm^2 in surface area and dried in a desiccator under vacuum. Fast-drying of $PbCl_2$ solution on the basal surfaces of muscovite resulted in a surface that was that was almost completely coated with precipitate having a leaflike morphology. a) Image where the cone-shaped islands are near the centers of the leaflike precipitates. b) Image where the leaflike precipitates are isolated with clear boundaries or are interspersed with smaller $PbCl_2$ clusters.

https://doi.org/10.1346/CCMN.1998.0460308 Published online by Cambridge University Press

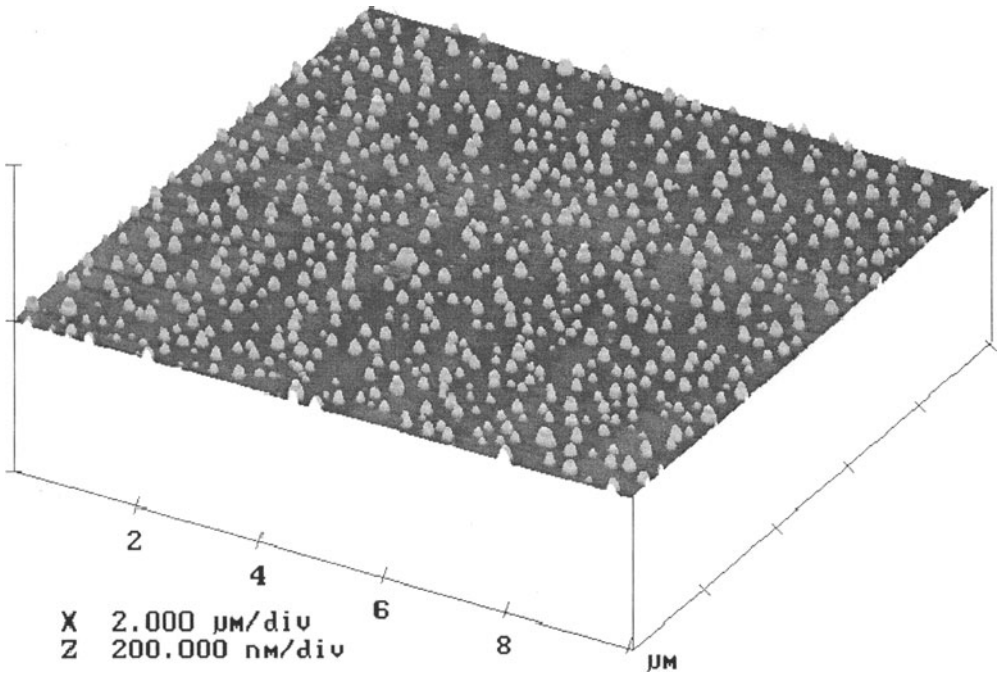

Figure 5. Precipitates of $PbCl_2$ on perfectly cleaved basal surfaces of muscovite (001 plane): 20 μL 5×10^{-4} *M* $PbCl_2$ solution pipetted onto a muscovite sample ~1 cm^2 in surface area and air-dried in a covered petri dish. Slower-drying process resulted in a surface covered with more isolated circular-shaped $PbCl_2$ precipitates.

concentric rings of precipitated $PbCl_2$ seen in Figures 6a and 6b may be explained as follows. As evaporation proceeds, the film of unsaturated $PbCl_2$ solution will eventually become discontinuous and break up into discrete circular droplets, due to the effect of surface tension. On further evaporation, the solution may become supersaturated and precipitation will eventually occur, resulting in the deposition of small crystalline $PbCl_2$ aggregates under the droplet. As time progresses, the size of the droplet will diminish; thus, the particles along the outer periphery will no longer be in contact with solution. The $PbCl_2$ crystals inside the droplet can be expected to grow with time as the droplet shrinks so that the crystals located at the center of the droplet will be the largest. In addition, there will be a diffusional mass transfer process, driven by crystal surface energy, which will cause large crystals to grow at the expense of smaller ones. This will have the effect of reducing the size and number of small crystalline deposits in the region between the outer crystalline deposits and the center of the droplet. Thus, the ring patterns of $PbCl_2$ precipitates as shown in Figures 6a and 6b might result.

SUMMARY

Precipitates of $PbCl_2$ were found on the basal surfaces, steps and edges of muscovite with precipitation preferentially occurring along the broken steps compared to the basal surfaces. This suggests that edges of the freshly cleaved muscovite are more reactive than the basal surfaces and that nucleation and precipitation reactions are likely initiated from the Pb^{2+} ions adsorbed at the terminal $Al\text{-}OH_2^{1/2+}$ or $Al\text{-}OH^{1/2-}$ groups on these edges. Precipitates of $PbCl_2$ were found to grow laterally at different spatial directions at the edge of the multiple muscovite layers. This was attributed to different orbital orientations of these terminal groups on the crystalline surfaces exposed at the edge. It was found that the edges of weathered muscovite are not as reactive as those on the freshly cleaved muscovite. It was observed that the morphology of $PbCl_2$ precipitates on basal surfaces is affected by the drying rate. These results are in agreement with other studies and showed that precipitation reactions on minerals surfaces play an important role in immobilizing heavy metals in soils and sediments. The role of precipitation reactions may have been underestimated in soils at arid and semiarid regions, where soils are subject to continuous wetting-drying cycles.

ACKNOWLEDGMENTS

We thank the late P. F. Low for directing our attention to the literature on Liesegang rings. We also wish to thank A. D. King of the University of Georgia for his helpful comments and suggestions on our manuscript and L. Akim of the National Research Council/U.S. Environmental Protection Agency, Athens, Georgia, for his assistance in computer graphics. This work was performed while the first named author held an NRC Research Associateship at Ecosystems Re-

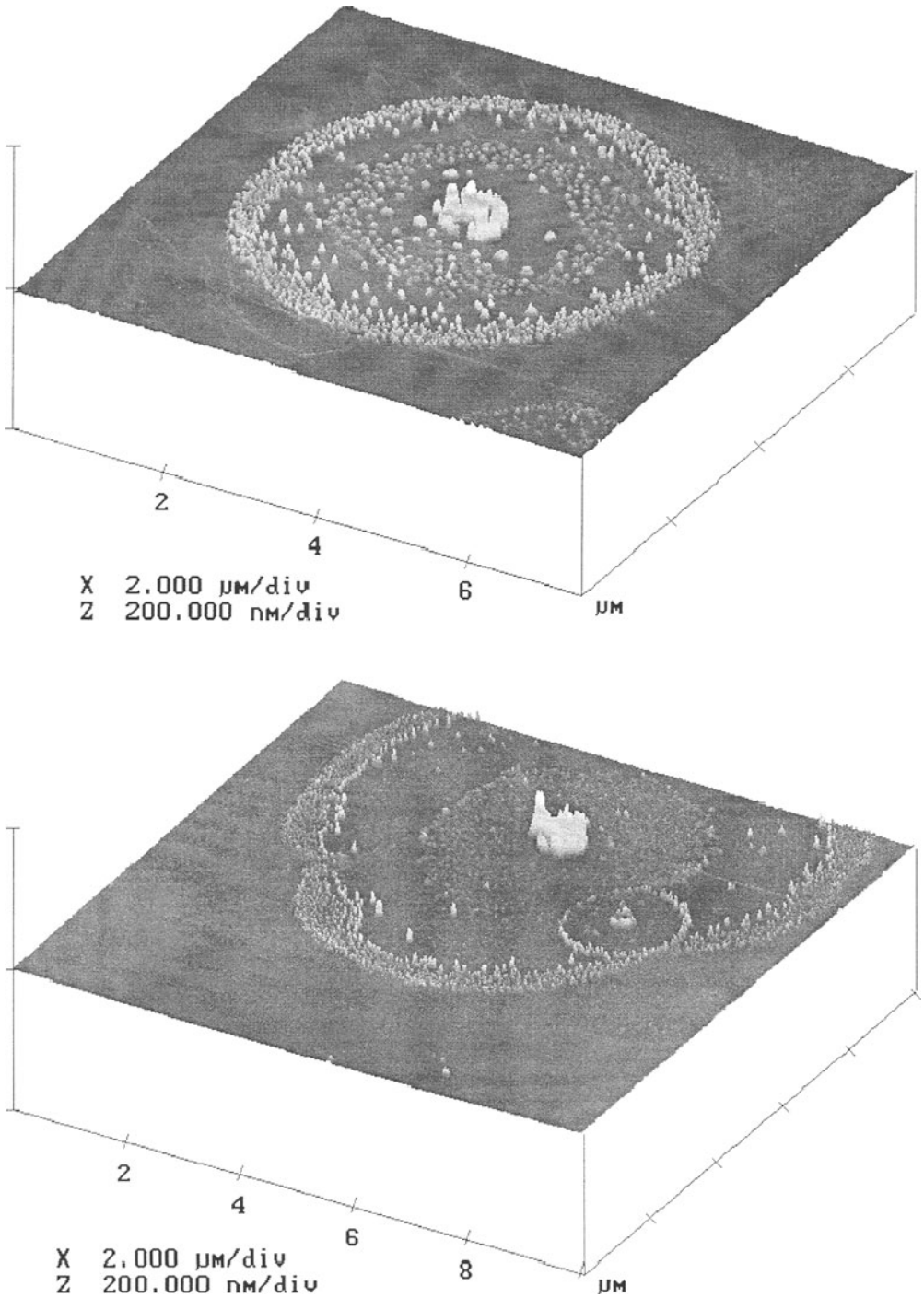

Figure 6. Precipitates of $PbCl_2$ on perfectly cleaved basal surfaces of muscovite (001 plane): 40 µL 5 × 10^{-5} *M* $PbCl_2$ solution pipetted onto a muscovite sample ~1 cm^2 in surface area and air-dried in a covered petri dish. Precipitates of $PbCl_2$ were often formed in a pattern of concentric rings. a) Image where the precipitates increase in size toward the center of the ring patterns. b) Image where a secondary ring pattern was formed inside the primary ring pattern.

https://doi.org/10.1346/CCMN.1998.0460308 Published online by Cambridge University Press

search Division, National Exposure Research Laboratory, US EPA, Athens, Georgia.

REFERENCES

Allison JD, Brown DS, Novo-Gradac KJ. 1991. MINTEQA2/PRODEFA2, A geochemical assessment model for environmental systems: Version 3.0 user manual. Athens, GA: US Environmental Protection Agency. EPA/600/3-91/021. 106 p.

Binnig G, Quate CF, Gerber C. 1986. Atomic force microscope. Phys Rev Lett 56:930–933.

Binnig G. 1992. Force microscopy. Ultramicroscopy 42–44: 7–15.

Bleam WF, McBride MB. 1985. Cluster formation versus isolated-site adsorption. A study of Mn(II) and Mg(II) adsorption on boehmite and goethite. J Colloid Interface Sci 103: 124–132.

Bosbach D, Rammersee W. 1994. *In situ* investigation of growth and dissolution on the (010) surface of gypsum by scanning force microscopy. Geochim Cosmochim Acta 58: 843–849.

Brodde A, Neddermeyer H. 1992. Nucleation and growth of Fe on Cu *(111)* in the monolayer range. Ultramicroscopy 42–44:556–561.

Cotton FA, Wilkinson G. 1988. Advanced inorganic chemistry, 5th edition. New York: J. Wiley. p 1455.

Davis JA, Hem JD. 1989. The surface chemistry of aluminum oxides and hydroxides. In: Sposito G, editor. The environmental chemistry of aluminum, Boca Raton, FL: CRC Pr. p 185–219.

Dibble WE Jr, Tiller WA. 1981. Non-equilibrium water/rock interactions. I. Model for interface-controlled reactions. Geochim Cosmochim Acta 45:79–92.

Dove PM, Hochella MF Jr. 1993. Calcite precipitation mechanisms and inhibition by orthosphate: *In situ* observations by scanning force microscopy. Geochim Cosmochim Acta 57:705–714.

Fendorf SE, Sparks DL, Fendorf M, Gronsky R. 1992. Surface precipitation reactions on oxide surfaces. J Colloid Interface Sci 148:295–298.

Fendorf SE, Li G, Gunter ME. 1996. Micromorphologies and stabilities of chromium (III) surface precipitates elucidated by scanning force microscopy. Soil Sci Soc Am J 60:99–106.

Henisch HK. 1988. Crystals in gels and Liesegang rings. New York: Cambridge Univ Pr. p 197.

Hochella MF Jr. 1990. Atomic structure, microtopography, composition, and reactivity of mineral surfaces. In: Hochella MF Jr, White AF, editors. Mineral-water interface geochemistry. Washington, DC: Mineral Soc Am. p 87–132.

Hochella MF Jr, Eggleston CM, Elings VB, Parks GA, Brown GE Jr, Wu CM, Kjoller K. 1989. Mineralogy in two dimensions: Scanning tunneling microscopy of semiconducting minerals with implications for geochemical reactivity. Am Mineral 74:1233–1246.

Hohl H, Stumm W. 1976. Interaction of Pb^{2+} with hydrous γ-Al_2O_3. J Colloid Interface Sci 55:281–288.

Jackson ML. 1964. Chemical composition of soils. In: Bear FE, editor. Chemistry of the soil. New York: Reinhold. p 71–141.

Jean GE, Bancroft GM. 1985. An XPS and SEM study of gold deposition at low temperatures on sulphide mineral surfaces: Concentration of gold by adsorption/reduction. Geochim Cosmochim Acta 49:979–987.

Jordan G, Rammersee W. 1996. Dissolution rates and activation energy for dissolution of brucite (001): A new method based on the microtopography of crystal surfaces. Geochim Cosmochim Acta 60:5055–5062.

Junta JL, Hochella MF Jr. 1994. Manganese (II) oxidation at mineral surfaces: A microscopic and spectroscopic study. Geochim Cosmochim Acta 58:4985–4999.

Lasaga, AC. 1981. The atomistic basis of kinetics: Deficits in minerals. In: Lasaga AC, Kirkpatrick RJ, editors. Kinetics of geochemical processes. Washington, DC: Mineral Soc Am. p 261–320.

Lee SY, Jackson ML. 1977. Surface charge density determination of micaceous minerals by ^{235}U fission particle track method. Clays Clay Miner 25:295–301.

O'Day PA, Brown GE Jr, Parks GA. 1994. X-ray absorption spectroscopy of cobalt (II) multinuclear surface complexes and surface precipitates on kaolinite. J Colloid Interface Sci 165:269–289.

Ohnesorge F, Binnig G. 1993. True atomic resolution by atomic force microscopy through repulsive and attractive forces. Science 260:1451–1456.

Radoslovich EW. 1975. Micas in macroscopic forms. In: Gieseking JE, editor. Soil components, vol. 2, Inorganic components. New York: Springer-Verlag. p 27–57.

Scheidegger AM, Lamble GM, Sparks DL. 1996. Investigation of Ni sorption on pyrophyllite: An XAFS study. Environ Sci Technol 30:548–554.

Stumm W, Morgan JJ. 1995. Aquatic chemistry: Chemical equilibria and rates in natural waters, 3rd edition. New York: J. Wiley. p 1022.

Weast RC, Astle MJ, editors. 1982. CRC handbook of chemistry and physics, 63rd edition. Boca Raton, FL: CRC Pr.

Weiser HB. 1935. Inorganic colloid chemistry, vol. 2. The hydrous oxides and hydroxides. New York: J. Wiley. p 429.

Zhang ZZ, Bailey GW. 1997. Precipitation/dissolution of lead compounds on surfaces of muscovite: An AFM study. Agronomy abstract; 1997 Annual ASA, CSSA, SSSA Meetings; Anaheim, CA. p 195.

(Received 4 February 1997; accepted 28 September 1997; Ms. 97-013)